UNIVERSIDAD AUTÓNOMA METROPOLITANA

03 de febrero de 2025

Dr. José Luis Gómez Olivares
Presidente del Consejo Divisional
P r e s e n t e.

Por medio de la presente, me permito solicitar un periodo sabático comprendido del 24 de marzo de 2025 al 23 de marzo de 2026, con base en el artículo 228 del RIPPA, que establece:

"El consejo divisional podrá atender los casos presentados fuera del plazo señalado en el artículo anterior, cuando medien circunstancias que a su propio juicio justifiquen la presentación extemporánea de las mismas."

Los motivos de esta solicitud son:

Inicio de un postdoctorado en innovación educativa en el mes de marzo, autofinanciado, con el propósito de fundamentar y concluir artículos de investigación educativa para su publicación. Cabe mencionar que este trimestre no cuento con carga académica.
Colaboración en una investigación sobre zonas de contacto a nivel celular en conjunto con el Instituto de Fisiología Celular de la UNAM, donde estamos finalizando experimentos y redactando un artículo científico.

Adjunto la Constancia Oficial de Servicios (Anexo 1) como parte de los requisitos para esta solicitud.

Atentamente

Dra. Carolina Campos Muñiz
Departamento de Ciencias de la Salud

UNIVERSIDAD AUTÓNOMA METROPOLITANA
Casa abierta al tiempo
4 - FEB. 2025
Unidad Iztapalapa
C.B.S.
Oficina Técnica de Consejo Divisional

Vo.Bo. Dr. Fernando Rivera Cabrera
Jefe del Departamento de Ciencias de la Salud

Casa abierta al tiempo

UNIVERSIDAD AUTÓNOMA METROPOLITANA
Unidad Iztapalapa

CRHIC.002.2025
Enero 08, 2025

Asunto: Constancia Oficial de Servicios

Consejo Divisional de Ciencias
Biológicas y de la Salud
Unidad Iztapalapa
P r e s e n t e

Por este conducto hago constar que la profesora **CAROLINA CAMPOS MUÑIZ** con número de empleado 18363 ingresó a esta Institución como Profesor de Tiempo Completo a partir del 20 de octubre de 1989, en el Departamento de Ciencias de la Salud de esta División y Unidad, *no habiendo disfrutado de licencia alguna.*

Disfrutó de los siguientes periodos de sabático:

del 19 de enero de 2004	al	18 de julio de 2005	(18 meses)
del 12 de abril de 2010	al	11 de abril de 2011	(12 meses)
del 23 de mazo de 2021	al	22 de marzo de 2022	(12 meses)

La profesora Campos tiene un tiempo acumulado de servicios de: 10 años, 05 meses, 18 días.

Cabe señalar que la profesora Campos para disfrutar de un nuevo periodo sabático deberá de ajustarse a lo señalado en el artículo 8 del acuerdo 01/90 UAM-SITUAM

A t e n t a m e n t e
Casa abierta al tiempo

Lic. Ciro Marcelo Díaz Rojas
Coordinador

UNIVERSIDAD AUTONOMA METROPOLITANA-I
RECURSOS HUMANOS

COORDINACIÓN DE RECURSOS HUMANOS
Avenida Ferrocarril San Rafael Atlixco, número 186, Colonia Leyes de Reforma 1A Sección, Alcaldía Iztapalapa,
Código Postal 09310, Ciudad de México
Tel. 5558-04-48-53
ciro@xanum.uam.mx

Plan de trabajo

A continuacion detallo las actividades que se realizaran durante el año sabático.

Investigación educativa en ciencias experimentales	
Elaboración del proyecto de posdoctorado. Durante el año, no son fechas definidas.	Requisito la universidad como conclusión del posdoctorado.
Se requiere el fundamento pedagógico que pide la revista y enviar para su publicación Marzo-mayo 2025	Title Raman simulator: a simple and didactic simulation of Raman signals from biological structures with Python (se requiere de la justificación pedagógica). Enviado a la revista Journal of chemical education, para su publicación se requiere la fundamentación pedagógica (Anexo 2a)
Diseñar el generar el programa de proteínas, así como concluir la escritura para su publicación. Junio-agosto 2025	Localization of proteins in cellular and cytosolic membranes, a didactic simulation with phyton (Anexo 2b). Este artículo esta en proceso se realizo en Matlab, nos suguierieron realizarlo en Phyton. Este trabajo se implemento con los alumnos de la UEA de estructura de proteínas mediante un trabajo co-elaborativo y cooperativo .
Diseñar las rubricas de evaluación educativa y realizar el análisis estadístico, así como concluir la escritura para enviar a la revista indicada para su publicación. Septiembre-diciembre 2025	Esquematización de la Célula: Un Enfoque Neurocientífico para el Aprendizaje. Se tienen avances de los diseños de organelos *ad doc* a la enseñanza mediante esquemas. Para este contexto me inscribí a un diplomado de prácticas educativas basadas en neurociencia para aprovechar el aprendizaje (Anexo 2c)
Investigación en ciencias Realizar los ensayos para identificar las zonas de contacto. Marzo-julio 2025	Por otro lado, estamos trabajando en colaboración con el laboratorio de Microscopia electrónica del Instituto de Fisiología Celular (IFC) de la UNAM en una revisión de zonas de contacto entre organelos. Con ellos estamos tomando las fotografías de las zonas de contacto entre organelos (Anexo 2d). Articulo: Zonas de contacto a nivel celular, en hepatocitos de rata.

Anexo 2a

Raman simulator: a simple and didactic simulation of Raman signals from biological structures with Python

Campos C.[a*], Acosta-García C.[b], Sato-Berrú R.[c], Moreno-Ruiz L.A.[d], Martínez H.[e], and Fernández F.J.[f]

[a]Department of Health Sciences, Universidad Autónoma Metropolitana Iztapalapa, Avenida Ferrocarril San Rafael Atlixco 186, Colonia Leyes de Reforma, 1A Sección, Iztapalapa, C.P. 09310, Mexico City, Mexico

[b]Department of Reproductive Biology, Universidad Autónoma Metropolitana Iztapalapa, Avenida Ferrocarril San Rafael Atlixco 186, Colonia Leyes de Reforma, 1A Sección, Iztapalapa, C.P. 09310, Mexico City, Mexico

[c]Institute of Applied Sciences and Technology, Universidad Nacional Autónoma de México, Circuito Exterior S/N, Ciudad Universitaria, A.P. 70-186, Coyoacán, C.P. 04510, Mexico City, Mexico

[d]Center for Nanosciences and Micro and Nanotechnologies, Instituto Politécnico Nacional, Av. Luis Enrique Erro S/N, Unidad Profesional Adolfo López Mateos, Zacatenco, Gustavo A. Madero, C.P. 07738, Mexico City, Mexico

[e]Institute of Physical Sciences, Universidad Nacional Autónoma de México, Av. Universidad s/n, Col. Chamilpa, Cuernavaca, Morelos, 62210, Mexico

[f]Department of Biotechnology, Universidad Autónoma Metropolitana-Iztapalapa, Avenida Ferrocarril San Rafael Atlixco 186, Colonia Leyes de Reforma, 1A Sección, Iztapalapa, C.P. 09310, Mexico City, Mexico

Running title: Raman simulator software for biological structures

***Corresponding author:** Campos C., caro@xanum.uam.mx

Abstract

This work shows the construction and use of a simple and didactic computational routine of Raman signals from biological structures. These signals or Raman bands were simulated in the free Python programming language. Likewise, diverse vibrational frequency tables characteristic of functional groups were used in the computational routine. Within the program are three examples of spectra, one corresponding to penicillin K (a secondary metabolite produced by *Penicillium* spp), a second that is the recombinant insulin, and a third of a single cell. These examples show a first approximation and coincidence to the Raman signals obtained using the Gaussian software and experimentally with a Raman system.

Keywords: biological tissues; educational software; insulin; penicillin; *Penicillium rubens*; Raman spectroscopy

Introduction

Raman spectroscopy is a measure of inelastic scattering, which allows studying molecular rotations and vibrations. It was discovered first by Chandrasekhara Venkata Raman in 1928 (receiving the Nobel Prize for his work in this field, together with K. S. P. Krishnan). Both authors described a "new type of secondary radiation" after some experiments involving the illumination of samples with sunlight focused through a lens. They observed a scattered light with a wavelength different from the original incident one; this scattering light is now known as Raman, which is induced by monochromatic light (generally from a laser directed to the cell): the photons interact with the sample and the energy can be lost (lower) (stokes-Raman) or gained (anti-stokes). This energy difference between the incident and the scattered photon corresponds to the required energy to excite a particular molecular vibration. The detection of these scattered photons produces a Raman spectrum that is a diagram of scattered intensity as a function of the energy difference between the incident and scattered photons and is obtained by pointing a monochromatic laser beam to the sample [1].

The Raman system is similar to most optical spectroscopic systems, consisting of three main components: light source, sample light supply and collection, and dispersive element with a detector (Fig. 1) [2]. The resulting spectra are characterized by having changes in the wave number (inverse of the wavelength expressed in cm^{-1}) from the incident frequency. The difference in frequency between the incident light and the scattered Raman light is called the Raman variation, which is unique to individual molecules, is measured by a machine detector, and is represented as 1/cm. Raman peaks are spectrally narrow in many cases and may be associated with the vibration of a particular chemical bond or different functional groups; therefore, each molecule has a unique fingerprint or spectrum according to the chemical bonds within it [3].

A Raman spectrum provides both qualitative and quantitative information at the molecular level of the analyzed samples. It has been used in various fields, such as materials, life sciences, the food and pharmaceutical industry, or for forensic [4] and biomedical applications, which has led to significant progress in the field of clinical evaluation. In the latter, spectroscopic techniques, including Raman spectroscopy, have been carried out in a series of tissues. Vibrational spectroscopic techniques are relatively simple, reproducible, non-destructive to tissue, and require only small amounts and concentrations of material (micrograms to nanograms) with minimal sample preparation. In addition, these techniques provide information at the molecular level, allowing the investigation of functional groups, bond types, and molecular conformations [5].

The vibrational Raman spectral bands are specific for each molecule, providing direct information about the biochemical composition. The bands are

relatively narrow, easy to resolve, and sensitive to molecular structure or conformation. In recent years, spectroscopic methods have covered a wide field of medical and biological studies. It is firmly believed that, in the studies related to spectroscopic techniques, the experimental procedure is reliable, and the characterization of the spectral positions of the peaks and their assignment, together with their detection and precise definition, are of crucial importance for the characterization of the structures. Several authors have used different techniques, but there seems to be a marked similarity in the spectral interpretation of compared areas in the reported spectra [6].

Raman spectroscopy is a method that overcomes some of the limitations of other current spectroscopic techniques. At the cellular level, it yields characteristic spectra, considering that a eukaryotic cell consists of 60 to 70% water and approximately 30% macromolecules such as proteins, nucleic acids (DNA and RNA), polysaccharides, lipids, and some inorganic salts and other small molecules. The result is a Raman spectrum with different chemical bands that provides a characteristic spectral fingerprint [7]. Some of the most common interesting vibrational modes in molecular biology are indicated in Table I [6,8–12].

In recent years, these non-invasive vibrational spectroscopic techniques have been used in scientific research, including biochemical analyses, allowing for the dynamic characterization in living organisms without the use of fluorescent agents [5]. It has also been used to characterize individual eukaryotic cells *in vivo* and *in vitro* [13,14], and even for studying a single cell [10,15–18].

This methodology has also been used to observe disease-induced molecular changes reflected in Raman spectra, leading to the possibility of highly specific fingerprints of the biochemical composition of cells and tissues, including related clinical investigations with malignancy and cancer detection [19]. This has attracted the attention of both clinical and non-clinical researchers [5,19,20]. In this sense, studies in various organs have focused on a common point: the need to establish a sensitive and specific early detection strategy for various diseases [2].

Raman scattering from biological samples is usually weak and is often superimposed on the background signal resulting from intracellular biocomponents. To overcome these drawbacks, surface-enhanced Raman scattering (SERS) is used, a technique developed to increase the signal by taking advantage of the interaction among molecules being investigated with metallic nanoparticle substrates [21,22]; typically, gold, silver, or platinum is used. Electromagnetic enhancement is considered the dominant contributor to most SERS processes [23,24]. Nearby or adsorbed molecules on the metal substrate increase in the Raman signal that can subsequently lead to an order of magnitude increase in signal intensity [23,25,26]. SERS has recently been used in samples with low concentration of molecules for many medical applications ranging from probing to obtaining Raman signals in living cells [26].

For the analysis of molecules, great softwares have been designed to study the behavior of molecular bonds that characterize different compounds, both organic and inorganic, such as Gaussian [27], which is a system of connected programs to execute a great variety of calculations. Among others, it can model the electronic structure, predicting molecular properties and chemical reactions, as well as molecular vibration frequencies and their relative intensities, which are useful for spectroscopic methods such as Raman and infrared. These structure calculation methods have been increasingly used in molecular and diagnostic design applications [28].

The objective of this work was to design software that contains a list of peaks (bands) of functional groups and links of biological structures that will allow the student to model spectra while being introduced to the knowledge of Raman spectroscopy in a simple way, as well as to know and interpret molecular vibrational spectra, following some examples.

Material and method

Sample processing. Single cell analysis

Fungal strains. The high penicillin-producing *Penicillium rubens* strain P2-32-T was used, obtained from the P2-32 strain [29] by amplification of the number of copies of the genes that code for the penicillin biosynthesis [30]

Liquid culture. Spores (10^6) of the strain were inoculated in 50 mL of a complex growth medium in 250-mL flasks, incubated at 25 °C and 250 rpm, for 24 h. After this time, 5 mL of the culture were inoculated into 250-mL flasks containing 45 mL of a complex fermentation medium (MFCP) and incubated at 25 °C and 250 rpm, for 24 and 48 h [31].

Transmission Electron Microscopy (TEM)

The mycelium of the strain sample was taken, fixed in 1.5% glutaraldehyde in PBS buffer at pH 7.2 for 24 h. The sample was subsequently washed with PBS and postfixed with 1% osmium tetraoxide for several hours. Subsequently, it was rinsed and dehydrated in a series of ethanol at gradual concentrations, ending with propylene oxide. The pre-inclusion was performed with a mixture of propylene oxide and epoxy resin at a 1:1 ratio for 24 h. Finally, the sample was embedded in epoxy resin for 48 h at 60 °C. Semi-thin sections, 200 nm in thickness were obtained [32].

Raman spectroscopy

The sections were placed on a pure silver substrate. Raman spectroscopy measurements were performed with a LabRam confocal micro-Raman spectrometer model HR800 (Horiba Jovin Yvon, Kyoto, Japan), equipped with an Olympus model BX41 microscope, placing the samples to be examined on its stage. A 532-nm laser was used as the excitation source, whose nominal power is

73.9 mW, which was attenuated with a neutral density filter (D3=I/1000), operating with a pinhole opening of 300 µm and a slit opening of 150 µm, with a 100X magnification objective. Measurements were made with 8 s of exposure in a spectral range of 100 - 3500 cm^{-1}. For the analysis of penicillin K (Penicillin K sodium salt, Merck & Co, Inc., Kenilworth, NJ, US) and recombinant insulin (Insulinex N isophane insulin, recombinant DNA origin, Pisa Biotec, Albany, NY, US), they were placed separately on a glass slide and the same protocol was followed as for semi-thin sections.

Raman software design

The development of this software was carried out following a prototype methodology, in the Python programming language, through the object-oriented programming paradigm.

1. Bands database

1a. A list was made with the frequencies corresponding to the bands of the functional groups [3,33,34], with their corresponding identifier (by using the SQLite 3 data manager and creating a file with a .db extension) (Fig. 2).

1b. Integer numbers were used for the identifiers and the bands. Text was used for the functional groups.

2. Interface development

The user interface was developed, using the Python PyQt5 library, for all the widgets through which the user will interact with the program, and the matplotlib library for displaying the data. Figure 3 shows the interface components described below:

2a. In the upper right part, there is a menu labeled "language" that allows selecting between English and Spanish, for the language of the main knobs (Figure 3a).

2b. The graphical interface consists of a combo box labeled "Number of compounds" where the number of functional groups to work with can be selected (Figure 3b), on the next line a text labeled "Molecule's name" is used to specify the name of the functional group whose peak will appear on the plot (Figure 3c).

2c. Below the latter, are 50 combo boxes in which the functional groups and peak intensity can be selected (Figure 3d).

2d. In the lower part are three knobs, the first labeled "Example of Vibrational Bonds" that opens a window where the example of Penicillin K is found, showing the vibrational bonds; the second labeled "Restart" used to restart a new exercise, and the third one labeled "Shift-Molecule" that opens a new window and displays options for searching wavelengths (Figure 3e).

2e. On the right side, a window is shown where the graphs will be displayed, the x-axis is the wave number that goes from 0 to 3800 indicated with the Raman shift units (cm^{-1}) and, on the y-axis, is the intensity from 0 to 10,000 (arbitrary units) (Figure 3g). At the bottom of the graph, is a toolbar to navigate, the Home knob to restart the initial configuration, the back and forward arrows zoom to the section to be analyzed, modifying the spacing and borders, changing the style and colors, and saving the graph as an image (Figure 3h). On the lower right side are the values of the graph that are obtained by placing the cursor on a specific point (Figure 3i).

2f. In the lower right part, three knobs are shown with examples of Raman spectra obtained as mentioned under M&M, the first labeled "Penicillin K Example" and "Insuline Example" with the chemical structure, respectively, and "Cell Example" with a cell image (Figure 4). The data obtained by spectroscopy are loaded into the software.

3. Software logic

Once the database and the graphical user interface were created, the logic of the program was worked on, which is based on two classes. The first is in charge of creating the window, the user interface, and the actions that will be carried out from the user's interaction with it. The second is the class in charge of the graph of the data selected by the user.

The first class has the following methods:

Window initialization: With parameters such as the size of the window, the position in which it is initialized, its name, and the icon.

The method of connection to the database: Through this, a query to the database is made. In addition, it displays how the data of the previously created database table were obtained.

Initialization of the graphical user interface: Creating all the knobs, text boxes, list boxes, and check box, all specified above.

Filling the combo box: Adding the name of the compounds (and/or links) to the dropdown list.

Loading sample data: Loading the data of the intensities and peaks stored in txt files and the images of the chemical structures.

Enabling the number of functional groups: Allowing to select the number of functional groups required by the user, and the intensity associated with them.

Obtaining the wave number: Generate arrays with the wave numbers of the selected functional groups and the associated intensities, as well as control variables for the display of the peaks on the graph and the name of the molecule.

Instantiate the second class passing it as parameters, arrays, and control variables.

Reset selection: Set everything that is selected to default values, to reset the selection.

Change language to Spanish: To change the language of the main knobs from English to Spanish.

Change language to English: To change the language of the main knobs from Spanish to English.

The second class used in the development of this software is called Canvas, and comprises two methods:

Generator of the array of intensities: From the sum of a positive and a negative exponential function around the peak of the Raman band of each functional group. In case of overlapping, the intensities are added.

Layout of the graph: Generates the final result of the graph with the data, name and limits of the axes, and title of the graph.

Software evaluation by students

The software was evaluated by 30 undergraduate students. First, they identified the vibrational frequencies of penicillin (video contained in the simulator software obtained by Gaussian). Later they were assigned the task of analyzing the vibrational frequencies of penicillin (Figure 3.3) and atorvastatin (Figure 3.1) in the help command. Once the links were identified, the students simulated several spectra of their choice and, at the end, they were asked to answer the questionnaire on the effectiveness of the software (SEQ), with 14 questions each with 3 options (Table II). This evaluation methodology allowed collecting quantitative and qualitative information on the software effectiveness. The reliability of the questionnaire was evaluated using the Cronbach's alpha test, which defines the descriptiveness and normality of the study variable (level of attitude towards the software), and performs a comparative analysis of the study variable using the Wilcoxon test.

Results

Software main window

The main window of the Raman simulator (Fig. 3) shows a toolbar at the top; the first knob corresponds to the language in both Spanish and English, the second is the appearance in two modes (sepia and dark tones), and the third is to help in discerning which submenu is displayed. In the first row is the software tutorial and

"about" indicates the version of the software and its creators (Fig. 3.1). In the same row is the window for the selection of the number of compounds (Fig. 3.2). In the column on the left side are two windows: the first displaying a total of 50 functional groups (chosen by wavelength, peak, or band), and the second window displays the intensity of the bands/compounds (Fig 3.3).

The lower part of the main window shows an example of the structure of penicillin, indicating the vibrational bonds and the wavelength of each compound (Fig. 3.4). The second row depicts the "reset" knob, which allows to clear the screen and start a new exercise (Fig. 3.5). The third row shows the wavelengths of different compounds (Fig. 3.6). In the panel on the right side is the toolbar that allows the student to start again, advance or revert functions, drag the figure, amplify the spectra, adjust the axes of the graph, adjust the data, and save the created spectrum (Fig. 3.7).

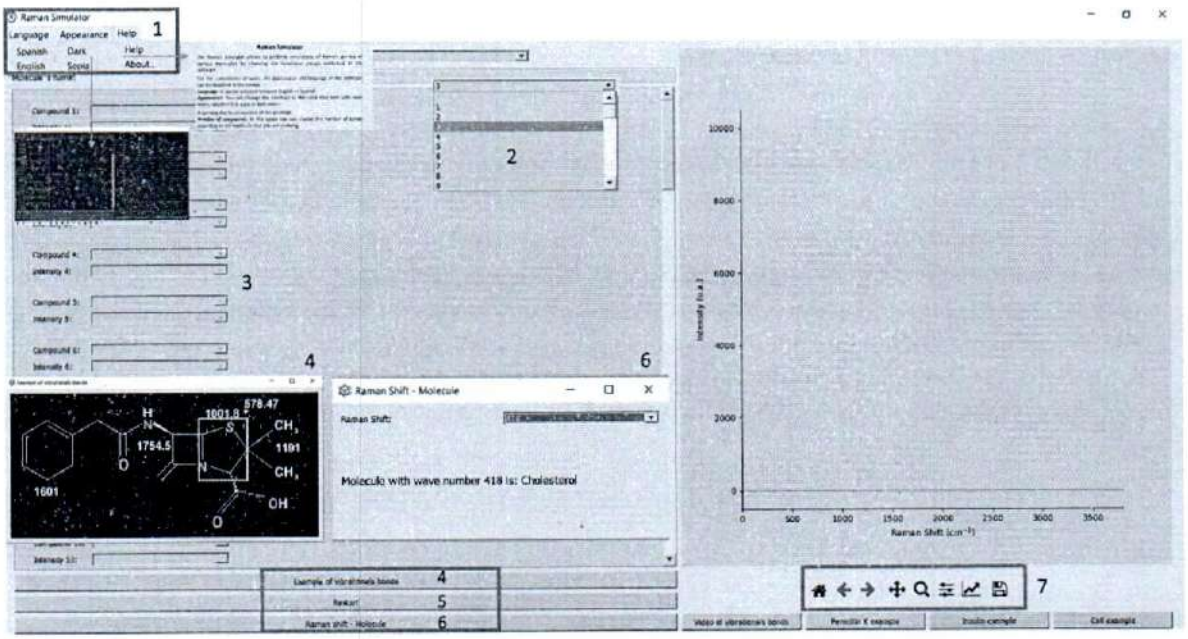

Figure 3

Below the toolbar are four windows (Fig. 4). The first shows the video of vibrational bonds of penicillin obtained by Gaussian (Fig. 4.1); the second knob shows the spectrum of penicillin K, whose results were compared with those reported by Zhang et al. [35]. The peaks of the characteristic functional groups of this molecule are indicated. The same figure shows the chemical structure obtained by Gaussian (Fig. 4.2). The third button shows the Raman spectrum of recombinant insulin, the peaks obtained by spectroscopy were compared with those reported by Ortiz et al. [36]. Below the spectrum, the amino acid sequence contained in the protein is shown (Fig. 4.3). The fourth button shows the Raman spectrum of a single cell whose

assigned bands are indicated on the graph; below this, the *P. rubens* cell micrograph obtained by TEM is shown (Fig. 4.4).

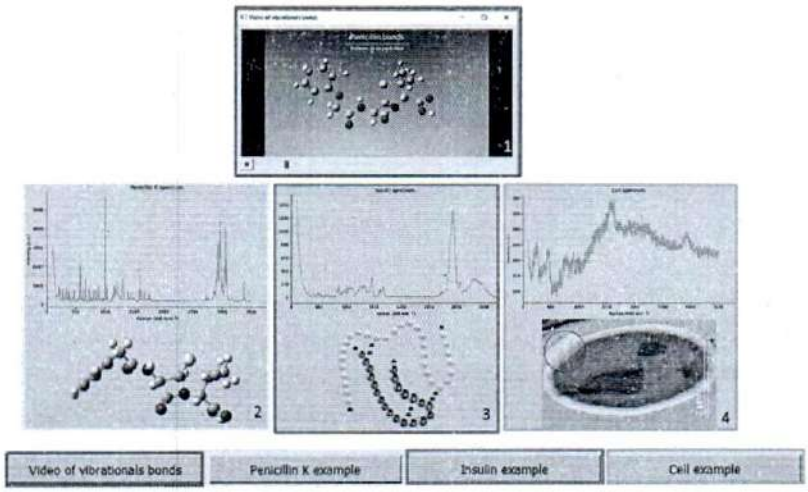

Figure 4

Figure 5 shows a spectrum simulated by three peaks, indicating the component and intensity of each peak. The spectrum obtained is shown in the right-hand panel; under this spectrum, the precise point of the graph coordinates can be known.

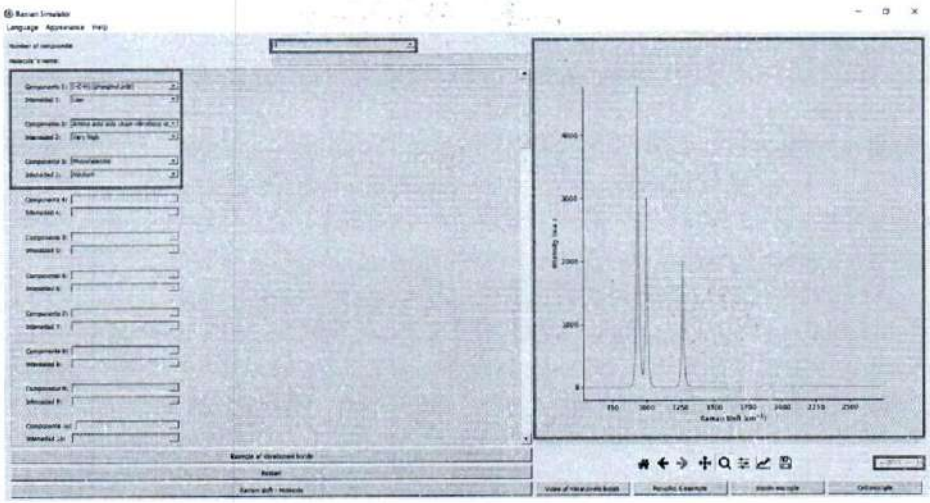

Figure 5

Statistical analysis of software relevance

The relevance and pedagogical usefulness studies of the Raman simulator were performed with a group of 30 students, using the SEQ instrument (Table II). Considering the structure of the instrument, a fixed score was chosen as the baseline or pretest (value 2.5) and the information collected from the questionnaire was added as a starting line or posttest on the full scale. The process began by observing the

reliability of the SEQ instrument, which was determined with the internal consistency method through Cronbach's Alpha coefficient. The questionnaire obtained an index of 0.745 of the information obtained from the 30 students, indicating that the instrument presents an acceptable reliability, being greater than 0.70. The normality analysis with the Shapiro-Wilk test ($p < 0.05$) showed that the variable does not present a normal distribution, so the nonparametric Wilcoxon signed-rank test will be used for one sample. In a first descriptive analysis, it was observed that the mean ($M = 2.70$) and median ($Me = 2.75$) of the students' attitude toward the software were higher than the baseline score (2.5).

As a second descriptive analysis, the total scores of the 30 subjects regarding their attitude toward the software were categorized into three groups: unfavorable attitude (scores from 14 to 23), low favorable (24-33), and favorable (34-42). The majority showed a favorable attitude toward the software (90.0%). On the other hand, three students (10.0%) were categorized at the unfavorable level. Because the above information is only descriptive, it was essential to corroborate it with the comparative analysis of the Wilcoxon signed-rank test for a sample. The result showed a significant increase in the attitude scores toward the software of the students ($Me = 2.75$) with respect to the baseline (2.5) when finding a p-value less than 0.05 ($z = 3.469$, $p < 0.05$). Therefore, it is concluded that there is a positive effect regarding the attitude toward the software in the study sample.

Discussion

The pedagogical foundation of this educational software lies in its ability to provide students with an efficient and effective tool to quickly characterize the structure and chemical composition of a sample, considering the statistical analysis shown in Table IV. Using concrete examples, such as the molecular vibrations video and the spectra of penicillin K and insulin, the software visually displays the functional groups present in each chemical structure and the Raman bands corresponding to these molecules. The latter allows students to understand, in a tangible and practical way, the concepts of Raman spectroscopy and its application in the analysis of molecules.

The intuitive and easy-to-use software's interface provides students with an enriching learning experience, allowing them to receive immediate feedback. This encourages their autonomous learning as they can actively explore and experiment with the software in a personalized way. Immediate feedback allows them to correct errors, adjust, and improve their understanding of Raman spectroscopy-related concepts.

In addition, the software provides the students with the necessary tools for the analysis of biological molecules. This is especially relevant in disciplines such as medicine, forensic sciences, pharmaceuticals, genetics, and nanotechnology, where the precise analysis of the structure and composition of molecules is

essential. The software issues a comprehensive database of vibrational bonds of molecules and compounds, allowing spectra with numerous peaks or bands to be generated and to perform qualitative or quantitative analyses quickly and orderly. It also provides students with valuable information for the characterization and understanding of the samples.

Conclusions

The results obtained for the feasibility evaluation of the Raman software (n=30) support the pedagogical justification of its implementation in an educational environment. The software promoted a deeper understanding of the concepts related to vibrational bonds and the interpretation of Raman spectra, which is attributed to its interactive and visual approach that facilitates the assimilation of content effectively. The software's ease of use and immediate feedback allowed the students to learn autonomously and correct errors in real time. These results support the educational relevance of Raman software, as it enhances teaching and learning by providing a stimulating and effective learning experience. By fostering interest, active participation, and the development of problem-solving skills, Raman software is a valuable tool for enriching education in spectroscopy and promoting greater student engagement.

Acknowledgments

We thank Ingrid Mascher for copy-editing the English version of the manuscript.

Funding

This research received no specific grant from any funding agency in the public, commercial, or not-for-profit sectors.

Declaration of Conflicting Interests

The authors declare that there is no conflict of interest.

ORCID iD

Campos C. https://orcid.org/0000-0003-2871-1173

Acosta-García C. https://orcid.org/0000-0002-3311-7833

Sato-Berrú R. https://orcid.org/0000-0002-6492-0004

Moreno-Ruiz L.A. https://orcid.org/0000-0002-1880-1258

Martínez H. https://orcid.org/0002-0695-3457

Fernández F.J. https://orcid.org/0000-0003-4676-1828

References

(1) Raman, C. v; Krishnan, K. S. A New Type of Secondary Radiation. *Nature* **1928**, *121* (3048), 501–502. https://doi.org/10.1038/121501c0.

(2) Pence, I.; Mahadevan-Jansen, A. Clinical Instrumentation and Applications of Raman Spectroscopy. *Chem Soc Rev* **2016**, *45* (7), 1958–1979. https://doi.org/10.1039/c5cs00581g.

(3) Talari, A. C. S.; Movasaghi, Z.; Rehman, S.; Rehman, I. ur. Raman Spectroscopy of Biological Tissues. *Appl Spectrosc Rev* **2014**, *50* (1), 46–111. https://doi.org/10.1080/05704928.2014.923902.

(4) Das, R. S.; Agrawal, Y. K. Raman Spectroscopy: Recent Advancements, Techniques and Applications. *Vib Spectrosc* **2011**, *57* (2), 163–176. https://doi.org/10.1016/j.vibspec.2011.08.003.

(5) Kong, K.; Kendall, C.; Stone, N.; Notingher, I. Raman Spectroscopy for Medical Diagnostics — From *in-Vitro* Biofluid Assays to *in-Vivo* Cancer Detection. *Adv Drug Deliv Rev* **2015**, *89*, 121–134. https://doi.org/10.1016/j.addr.2015.03.009.

(6) Movasaghi, Z.; Rehman, S.; Rehman, I. U. Raman Spectroscopy of Biological Tissues. *Appl Spectrosc Rev* **2007**, *42* (5), 493–541. https://doi.org/10.1080/05704920701551530.

(7) Naumann, D. FT-Infrared and FT-Raman Spectroscopy in Biomedical Research. *Appl Spectrosc Rev* **2001**, *36* (2–3), 239–298. https://doi.org/10.1081/asr-100106157.

(8) Barth, A.; Zscherp, C. What Vibrations Tell about Proteins. *Q Rev Biophys* **2002**, *35* (4), 369–430. https://doi.org/10.1017/s0033583502003815.

(9) de Gelder, J.; de Gussem, K.; Vandenabeele, P.; Moens, L. Reference Database of Raman Spectra of Biological Molecules. *Journal of Raman Spectroscopy* **2007**, *38* (9), 1133–1147. https://doi.org/10.1002/jrs.1734.

(10) Shen, Y.; Hu, F.; Min, W. Raman Imaging of Small Biomolecules. *Annu Rev Biophys* **2019**, *48* (1), 347–369. https://doi.org/10.1146/annurev-biophys-052118-115500.

(11) Short, K. W.; Carpenter, S.; Freyer, J. P.; Mourant, J. R. Raman Spectroscopy Detects Biochemical Changes Due to Proliferation in Mammalian Cell Cultures. *Biophys J* **2005**, *88* (6), 4274–4288. https://doi.org/10.1529/biophysj.103.038604.

(12) Yu, C.; Gestl, E.; Eckert, K.; Allara, D.; Irudayaraj, J. Characterization of Human Breast Epithelial Cells by Confocal Raman Microspectroscopy. *Cancer Detect Prev* **2006**, *30* (6), 515–522. https://doi.org/10.1016/j.cdp.2006.10.007.

(13) Caspers, P. J.; Lucassen, G. W.; Wolthuis, R.; Bruining, H. A.; Puppels, G. J. *In Vitro* and *in Vivo* Raman Spectroscopy of Human Skin. *Biospectroscopy* **1998**, *4* (S5), S31–S39. https://doi.org/10.1002/(sici)1520-6343(1998)4:5+<s31::aid-bspy4>3.0.co;2-m.

(14) Saif, F. A.; Yaseen, S. A.; Alameen, A. S.; Mane, S. B.; Undre, P. B. Identification and Characterization of *Aspergillus* Species of Fruit Rot Fungi Using Microscopy, FT-IR, Raman and UV–Vis Spectroscopy. *Spectrochim Acta A Mol Biomol Spectrosc* **2021**, *246*, 119010. https://doi.org/10.1016/j.saa.2020.119010.

(15) Smith, R.; Wright, K. L.; Ashton, L. Raman Spectroscopy: An Evolving Technique for Live Cell Studies. *Analyst* **2016**, *141* (12), 3590–3600. https://doi.org/10.1039/c6an00152a.
(16) Downes, A.; Mouras, R.; Bagnaninchi, P.; Elfick, A. Raman Spectroscopy and CARS Microscopy of Stem Cells and Their Derivatives. *Journal of Raman Spectroscopy* **2011**, *42* (10), 1864–1870. https://doi.org/10.1002/jrs.2975.
(17) Mikoliunaite, L.; Rodriguez, R. D.; Sheremet, E.; Kolchuzhin, V.; Mehner, J.; Ramanavicius, A.; Zahn, D. R. T. The Substrate Matters in the Raman Spectroscopy Analysis of Cells. *Sci Rep* **2015**, *5*, 13150. https://doi.org/10.1038/srep13150.
(18) Schie, I. W.; Huser, T. Methods and Applications of Raman Microspectroscopy to Single-Cell Analysis. *Appl Spectrosc* **2013**, *67* (8), 813–828. https://doi.org/10.1366/12-06971.
(19) Auner, G. W.; Koya, S. K.; Huang, C.; Broadbent, B.; Trexler, M.; Auner, Z.; Elias, A.; Mehne, K. C.; Brusatori, M. A. Applications of Raman Spectroscopy in Cancer Diagnosis. *Cancer and Metastasis Reviews* **2018**, *37* (4), 691–717. https://doi.org/10.1007/s10555-018-9770-9.
(20) Fălămaş, A.; Rotaru, H.; Hedeşiu, M. Surface-Enhanced Raman Spectroscopy (SERS) Investigations of Saliva for Oral Cancer Diagnosis. *Lasers Med Sci* **2020**, *35* (6), 1393–1401. https://doi.org/10.1007/s10103-020-02988-2.
(21) Moskovits, M. Surface-Enhanced Raman Spectroscopy: A Brief Retrospective. *Journal of Raman Spectroscopy* **2005**, *36* (6–7), 485–496. https://doi.org/10.1002/jrs.1362.
(22) Schlücker, S. SERS Microscopy: Nanoparticle Probes and Biomedical Applications. *ChemPhysChem* **2009**, *10* (9–10), 1344–1354. https://doi.org/10.1002/cphc.200900119.
(23) Xie, W.; Schlücker, S. Medical Applications of Surface-Enhanced Raman Scattering. *Physical Chemistry Chemical Physics* **2013**, *15* (15), 5329. https://doi.org/10.1039/c3cp43858a.
(24) Muehlethaler, C.; Leona, M.; Lombardi, J. R. Review of Surface Enhanced Raman Scattering Applications in Forensic Science. *Anal Chem* **2015**, *88* (1), 152–169. https://doi.org/10.1021/acs.analchem.5b04131.
(25) Kambhampati, P.; Child, C. M.; Foster, M. C.; Campion, A. On the Chemical Mechanism of Surface Enhanced Raman Scattering: Experiment and Theory. *J Chem Phys* **1998**, *108* (12), 5013–5026. https://doi.org/10.1063/1.475909.
(26) Kneipp, J.; Kneipp, H.; McLaughlin, M.; Brown, D.; Kneipp, K. *In Vivo* Molecular Probing of Cellular Compartments with Gold Nanoparticles and Nanoaggregates. *Nano Lett* **2006**, *6* (10), 2225–2231. https://doi.org/10.1021/nl061517x.
(27) Frisch, M.; Trucks, G.; Schlegel, H.; Gill, P.; Johnson, B.; Robb, M.; Cheeseman, J.; Keith, T.; Petersson, G.; Montgomery, J.; Raghavachari, K.; Al-Laham, M.; Zakrzewski, V.; Ortiz, J.; Foresman, J.; Cioslowski, J.; Stefanov, B.; Challacombe, M.; Peng, C.; Ayala, P.; Chen, W.; Wong, M.; Andres, J.; Replogle, E.; Gomperts, R.; Martin, R.; Fox, D.; Binkley, J.; Defrees, J.; Baker, J.; Stewart, J.; Head-Gordon, M.; Gonzalez, C.; Pople, J. *Gaussian 94, Revision D*; Gaussian, Inc.: Pittsburgh, 1995.
(28) McClain, B. L.; Clark, S. M.; Gabriel, R. L.; Ben-Amotz, D. Educational Applications of Infrared and Raman Spectroscopy: A Comparison of Experiment and Theory. *J Chem Educ* **2000**, *77* (5), 654. https://doi.org/10.1021/ed077p654.

(29) Barrios-González, J.; Castillo, T. E.; Mejía, A. Development of High Penicillin Producing Strains for Solid State Fermentation. *Biotechnol Adv* **1993**, *11* (3), 525–537. https://doi.org/10.1016/0734-9750(93)90021-e.
(30) Campos, C.; Fernández, F. J.; Sierra, E. C.; Fierro, F.; Garay, A.; Barrios-González, J. Improvement of Penicillin Yields in Solid-State and Submerged Fermentation of *Penicillium Chrysogenum* by Amplification of the Penicillin Biosynthetic Gene Cluster. *World J Microbiol Biotechnol* **2008**, *24* (12), 3017–3022. https://doi.org/10.1007/s11274-008-9846-8.
(31) Somerson, N. L.; Demain, A. L.; Nunhelmer, T. D. Reversal of Lysine Inhibition of Penicillin Production by α-Aminoadipic or Adipic Acid. *Arch Biochem Biophys* **1961**, *93* (2), 238–241. https://doi.org/10.1016/0003-9861(61)90255-7.
(32) Spector, D.; Goldman, R.; Leinwand, L. *Cells: A Laboratory Manual*; Cold Spring Harbor Laboratory Press: New York, 1998.
(33) Clemens, G.; Hands, J. R.; Dorling, K. M.; Baker, M. J. Vibrational Spectroscopic Methods for Cytology and Cellular Research. *Analyst* **2014**, *139* (18), 4411–4444. https://doi.org/10.1039/c4an00636d.
(34) Palonpon, A. F.; Ando, J.; Yamakoshi, H.; Dodo, K.; Sodeoka, M.; Kawata, S.; Fujita, K. Raman and SERS Microscopy for Molecular Imaging of Live Cells. *Nat Protoc* **2013**, *8* (4), 677–692. https://doi.org/10.1038/nprot.2013.030.
(35) Zhang, L.; Jin, Y.; Mao, H.; Zheng, L.; Zhao, J.; Peng, Y.; Du, S.; Zhang, Z. Structure-Selective Hot-Spot Raman Enhancement for Direct Identification and Detection of Trace Penicilloic Acid Allergen in Penicillin. *Biosens Bioelectron* **2014**, *58*, 165–171. https://doi.org/10.1016/j.bios.2014.02.052.
(36) Ortiz, C.; Zhang, D.; Xie, Y.; Davisson, V. J.; Ben-Amotz, D. Identification of Insulin Variants Using Raman Spectroscopy. *Anal Biochem* **2004**, *332* (2), 245–252. https://doi.org/10.1016/j.ab.2004.06.013.

TABLES

Table I. Peak assignments for molecular Raman vibrations and related biomolecules

Vibrational mode	**Frequency cm^{-1}**	**Description**
Molecular bond	**Raman shift**	**Biomolecule**
CH_3	2930	Proteins (symmetric stretch)
CH_2	2854	Fatty acids, lipids, proteins (asymmetric stretch)
C-H stretching	2800-3020	C-H stretching mode
C=O stretching	1745	C=O stretching, ester group of lipids and phospholipds
C=O	1739	Esters, phospholipids, esterified fatty acids (stretching)

C=C	1668	Protein, α-helix of amide I, unsaturated fatty acids (stretching)
Amide I	1655	C=O stretching mode, peptide linkage
DNA/RNA	1570-1580	C=C stretching, purine bases
CH_2	1444	Fatty acids, lipids, proteins (bending and scissoring)
CH_2 and CH_3	1425-1475	Anti-symmetric methyl and methylene deformation
CH	1342	DNA–RNA (G) (deformation)
$\delta(CH_2)$	1303	Twisting, wagging, protein, fatty acids (twisting, wagging)
Amide III	1260-1350	Coupled C-H, N-H deformation modes, peptide backbone
PO_2-	1095	Symmetric stretching mode of phosphate ester, DNA, RNA, phospholipids
δ(C-H)	1003	Phenylalanine protein
Phenylalanine	1002	Symmetric stretching (ring breathing) mode of phenyl group
DNA/RNA (U, T, C) O-P-O	785	Pyramidine ring breathing (ring-breathing mode)

503
504

505 **Table II.** Questionnaire on the effectiveness of the software (SEQ).

1. Do you consider that the content of the software is clear and understandable in relation to the vibrations of molecules?
2. Do you find that the software provides an adequate introduction to the subject of vibrations of molecules?
3. Does the software use examples and case studies that facilitate understanding of molecular vibration concepts?
4. Do you think that the software presents the concepts in a sequential and organized way, allowing a logical progression in learning?
5. Do you find that the software uses an accessible and adequate language for the level of knowledge of the users?
6. Does the software include interactive activities that encourage participation and active learning?
7. Do you think that the software presents challenging exercises and problems that allow you to apply the concepts learned?
8. Does the software offer immediate feedback and detailed explanations for mistakes made in the exercises?
9. Do you find that the software uses visual aids, such as graphics or animations, to improve the understanding of the concepts of molecular vibrations?
10. Does the software provide tools to explore and visualize the vibrations of molecules interactively?
11. Do you think that the software motivates interest and curiosity in the subject of molecular vibrations?
12. Does the software include additional resources, such as links to articles or videos, that complement the main content and enrich learning?
13. Do you find that the software presents an intuitive and easy-to-use navigation structure?
14. Do you consider that the software is suitable for different levels of knowledge, from beginners to more advanced users in the field of molecular vibrations?

506

507

FIGURE LEGENDS

Figure 1. Block diagram of a Raman spectroscopy system: 1) microscope, 2) sample interface, 3) filter, 4) grating, 5) CCD detector, 6) spectrograph/dispersive element, 7) system control and feedback interface, 8) diode laser.

Figure 2. Spectral assignments for Raman cellular spectra.

Figure 3. Main window of the Raman simulator software. a. Language, appearance, and help. Number of compounds, c. molecule´s name, d. compound and intensity, e. vibrational bonds, f. example of the vibrational bonds, restart, and Raman shift-molecule.

Figure 4. Raman simulator software, right panel: (1) video of vibrational bonds, (2) penicillin K example, (3) insulin example, (4) cell example.

Figure 5. Raman simulator software, left panel: components and intensity. Central window: number of compounds. Right panel: Raman spectrum.

Anexo 2b

UBICACIÓN DE PROTEÍNAS: UN MODELO SIMPLE Y DIDÁCTICO CON MATLAB APP DESIGNER

[1]Laboratorio Biología estructural y funcional. Depto. Ciencias de la Salud UAM-I.
[2]Licenciatura en biología, División de Ciencias Biológicas y de la Salud. UAM-I
[3]Laboratorio de Química, Departamento de Química UAM-I
[4] Laboratorio de metabolitos Departamento de Biotecnología

Introducción

Las proteínas son las biomoléculas más importantes en la que se sustenta la vida están conformadas por 20 tipos de aminoácidos (a.a) diferentes, cada uno de los cuales tiene propiedades químicas distintas. Una proteína está formada por una larga cadena no ramificada de estos a.a, cada uno de los cuales está unida a su vecino mediante un enlace covalente llamado enlace peptídico. Por ello las proteínas también se les conoce como polipéptidos (Stollar y Smith., 2020). Cada tipo de proteína tiene una secuencia única de a.a por tal motivo el proteoma eucariótico consta de miles de proteínas diferentes. Los cambios en las condiciones de desarrollo, ambientales o metabólicas pueden inducir una remodelación considerable del proteoma (Brocchieri y Karlin., 2005).

Las proteínas son máquinas moleculares versátiles que controlan y ejecutan prácticamente todos los procesos celulares. Se sintetizan en un proceso de varias etapas que requiere la transferencia de información del ADN al ARN y finalmente al polipéptido (**Figura 1**). La síntesis de proteínas es inherentemente propensa a errores. Una célula de mamífero típica expresa más de 10 000 proteínas estructural y funcionalmente diversas, con números de copias que varían desde unas pocas moléculas hasta millones (Beck et al., 2011). Para alcanzar su estado funcional, las proteínas generalmente deben plegarse en estructuras tridimensionales apropiadas, ensamblarse, localizarse en compartimentos celulares específicos y existir en concentraciones apropiadas. Esta es una tarea enorme para la célula: en conjunto, las proteínas dedicadas a funciones relacionadas con el ciclo de vida del proteoma (traducción, elongación, plegamiento y proteólisis) constituyen un notable 10% de la masa del proteoma; con un 3% dedicado al plegamiento de proteínas (Muller et al., 2020).

Figura 1. Síntesis de proteínas. En una célula eucariota. Una vez que el ARNm sale del núcleo, viaja a un ribosoma. Aquí, el ribosoma lee la cadena de codones en la cadena de ARNm y luego el ARNt transporta los aminoácidos correspondientes al ribosoma en la secuencia exacta. Las proteínas en el citoplasma pueden ingresar a la vía secretora (SP), y dirigirse a otros organelos de la vía no secretora (nSP) o permanecer en el citoplasma (Vitale y Denecke, 1999). Las proteínas se trasladan al retículo endoplásmico (ER) mediante un mecanismo de cotraducción que implica la interacción en el citosol de un péptido señal N-terminal. La vía SP, o un dominio transmembrana, con una partícula de reconocimiento de señal (SRP). SRP dirige la proteína a un receptor de SRP localizado en el RE que, junto con un complejo translocón localizado en el RE (complejo Sec61), inicia la translocación al RE (Osborne et al., 2005 ; Shan y Walter, 2005). Luego, las proteínas secretoras se transportan a través del aparato de Golgi, para clasificarse y dirigirse al espacio extracelular o a los compartimentos endomembranosos posteriores (membrana plasmática, vacuolas en levaduras y plantas, lisosomas en animales, etc.).

Las proteínas cumplen una amplia diversidad de funciones dentro de los distintos compartimentos celulares. La función de una proteína depende del compartimento u orgánulo donde se encuentre, así como de su estructura, ya que proporciona un contexto fisiológico para su función. Para comprender completamente su función, es esencial explorar tanto su estructura como la localización subcelular (Stollar y Smith, 2021). Se han descrito al menos diez localizaciones subcelulares de proteínas en eucariotas, varias de las cuales pueden subdividirse en compartimentos intraorgánicos (Figura 2) y en procariotas, en el espacio intracelular y en membrana plasmática (**Figura 3**). Conocer la localización subcelular de las proteínas es una tarea esencial que ha sido ampliamente estudiada en bioinformática (Emanuelsson *et al.* , 2007 ; Imai y Nakai, 2010 ; Wan y Mak, 2015).

Figura 2. Célula eucariota: ubicación subcelular de algunas proteínas.

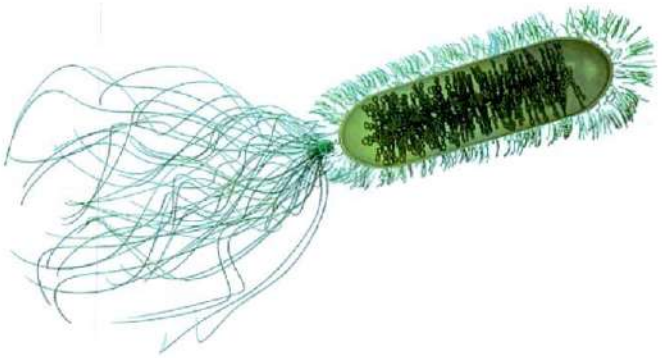

Figura 3. Célula eucariota. Ubicación subcelular de las proteínas

Ubicación por organelo

Objetivo

Programar una interfaz gráfica de usuario (GUI) que despliega la localización de las proteínas a nivel celular y de secreción en una interfaz amigable que permite al usuario relacionar el nombre, estructura con la ubicación celular o extracelular.

MATERIAL Y MÉTODO

A partir de una base de datos de 200 proteínas: nombre, estructura, localización celular y de secreción, se creó un directorio, se programó una GUI utilizando la plataforma de MATLAB App Designer. Al iniciar la aplicación, el programa carga la base de datos que contiene la ubicación de cada proteína y mediante un algoritmo de búsqueda en el listado, puede relacionar fácilmente la opción seleccionada con la información correspondiente. Las imágenes 3D fueron creadas en el programa (software) informático blender.

Resultados

El programa consiste en una sola ventana que incluye un botón de inicio que habilita el listado de proteínas en orden alfabético; al seleccionar una de las opciones, el programa ubica la proteína con su análogo, se abre una ventana emergente en donde se muestra la imagen de la célula en la que se resalta el organelo o citososl para conocer la ubicación celular del lado derecho se muestra la estrucura de la proteína.

Figura 4. Célula eucariota que muestra los lisosomas resaltados en color morado que se diferencia del resto de los organelos del lado derecho en el recuadro amarillo se muestra la proteína.

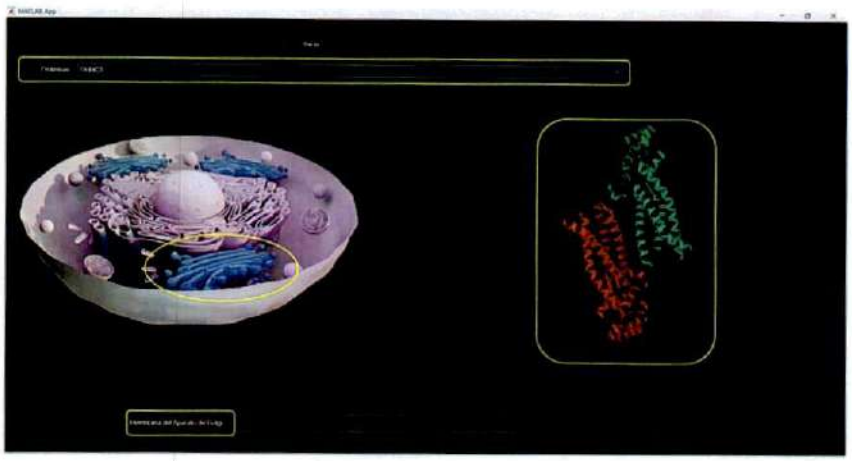

Figura 4. Célula eucariota que muestra el aparato de Golgi resaltados en color azul que se diferencia del resto de los organelos del lado derecho en el recuadro amarillo se muestra la proteína.

Discusión

El software didáctico muestra la localización de las proteínas así como su estructura, se realizo con la premisa de relacionar localización y estructura de la proteínas a nivel celular, se conoce que la localización subcelular influye de manera critica en la función de las proteínas, durante la sintesis proteica la célula tiene mecanismos eficiente de direccionamiento de cada proteina a la ubicación.

Este software es un primer acercamiento para que los alumnos conozcan la localización de algunas proteína en un esquema 3D que le sea significativo considerando el número de organelos y las sublocalizaciones habría varios miles de tipos diferentes de proteína, en este software se consideraron solo 200 proteínas suficientes para conocer las sublocalizaciones en las células eucariotas y de las procariotas.

Las células procariotas al ser más pequeñas con un mecanismo de regulación menos complejo al de la eucariotas es relativamente más sencillo de conocer la localización ya que solo identificaríamos las proteínas en la membrana plasmática y en el citosol, pero igualmente valioso conocer la localización de las proteínas en estos organismos.

Una de las desventajas que tiene los software de predicción es que las localización se predice por porcentajes y una proteína que es de secreción puede verse reflejada en otros lugares de la célula, dado que al ser sintetizada al interior celular es posible encontarla tanto en el RER y aparato de golgi, ya que deben pasar a estos organelos para que sufran las modificaciones porstraduccionales y sean funcionales.

Referencias

1. Beck M., Schmidt A., Malmstroem J., Claassen M., Ori A., Szymborska A., et al. (2011). The quantitative proteome of a human cell line. *Mol. Syst. Biol.* 7 (1), 549. 10.1038/msb.2011.82
2. Brocchieri, L., & Karlin, S. (2005). Protein length in eukaryotic and prokaryotic proteomes. *Nucleic acids research, 33*(10), 3390–3400. https://doi.org/10.1093/nar/gki615
3. Cline K., Henry R. Import and routing of nucleus-encoded chloroplast proteins. Annu. Rev. Cell. Dev. Biol. 1996;12:1–26.
4. Lee M.C. Bi-directional protein transport between the ER and Golgi. Annu. Rev. Cell Dev. Biol. 2004;20:87–123.
5. Neumann U. Protein transport in plant cells: in and out of the Golgi. Ann. Bot. 2003;92:167–180.
6. Muller J. B., Geyer P. E., Colaco A. R., Treit P. V., Strauss M. T., Oroshi M., et al. (2020). The proteome landscape of the kingdoms of life. *Nature* 582 (7813), 592–596. 10.1038/s41586-020-2402-x
7. Osborne, A. R., Rapoport, T. A., and van den Berg, B. (2005). Protein Translocation by the Sec61/SecY Channel. *Annu. Rev. Cel Dev. Biol.* 21, 529–550. doi:10.1146/annurev.cellbio.21.012704.133214
8. Shan, S.-o., and Walter, P. (2005). Co-translational Protein Targeting by the Signal Recognition Particle. *FEBS Lett.* 579 (4), 921–926. doi:10.1016/j.febslet.2004.11.049
9. Stollar, E. J., & Smith, D. P. (2020). Uncovering protein structure. *Essays in biochemistry, 64*(4), 649–680. https://doi.org/10.1042/EBC20190042

Anexo 2c

Esquemática y modelado celular

Arquitectura

"Ver" el mundo microscópico por medio de la esquemática modelos y modelado

La célula es una estructura altamente compleja y organizada, aún cuando sea de un organismo unicelular o de uno pluricelular. De acuerdo con el tejido u órgano su forma difiere, misma que esta relacionada con su función. Se ha esquematizado cada estructura para su mejor entendimiento de acuerdo con los avances del conocimiento de la célula. El objetivo de este trabajo fue diseñar una imagen representativa de la célula eucarionte en 3D y realizar un esquema de modelado de la membrana con el fin de ser conceptualizada mediante el texto y la esquemática. Si se estudia la célula del exterior, la primera ultraestructura que observamos es la membrana plasmática (MP), al interior como control celular encontramos al núcleo, su forma depende del molde de la célula, la función de este organelo es transportar macromoléculas como el RNAm hacia el Retículo endoplasmático rugoso (RER), en donde se lleva a cabo la síntesis de proteínas, cerca del RER se observa al Aparato de Golgi (AG), las proteínas recién sintetizadas en el RER sufren un proceso de maduración en el AG. Siguiendo el sistema de endomembranas (RER y AG), el Retículo endoplasmático liso (REL) es un organelo formado por una serie de tubos en el que lleva a cabo la síntesis de lípidos y algunas hormonas, así como de la detoxificación de sustancias tóxicas. Los peroxisomas tienen una forma esférica, cuya principal función es degradar el peróxido de hidrógeno, otro organelo similar son los lisosomas que degradan virus, bacterias y organelos viejos mediante enzimas. Otro organelo importante para la célula es la mitocondria que adopta su forma dependiendo del momento de la división independiente a la división nuclear, ya que ellas contienen su propia maquinaria para realizar este proceso (DNA), su función es generar energía química para la célula.

Palabras clave: Célula, esquemática, organelos, modelado.

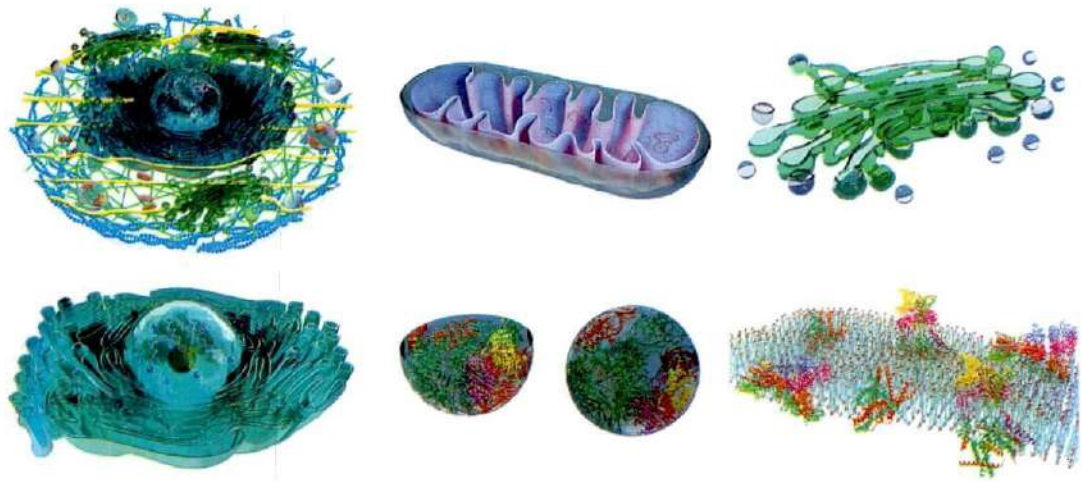

Casa abierta al tiempo
UNIVERSIDAD AUTÓNOMA METROPOLITANA

FI-DRH-20 / 12182013

SOLICITUD DE PERIODO SABÁTICO

UNIVERSIDAD AUTÓNOMA METROPOLITANA UNIDAD IZTAPALAPA

FECHA DE ELABORACIÓN	DÍA	MES	AÑO
	4	02	2025

DIRECTOR DE LA DIVISIÓN DE: CIENCIAS BIOLÓGICAS Y DE LA SALUD DE LA UNIDAD IZTAPALAPA

APELLIDO PATERNO	APELLIDO MATERNO	NOMBRE (S)	NÚM. DE EMPLEADO
CAMPOS	MUÑIZ	CAROLINA	18363

CATEGORÍA Y NIVEL: TITULAR C

UNIDAD	DIVISIÓN	DEPARTAMENTO
IZTAPALAPA	CIENCIAS BIOLÓGICAS Y DE LA SALUD	CIENCIAS DE LA SALUD

FECHA DE INGRESO A LA UAM COMO PERSONAL ACADÉMICO

DÍA	MES	AÑO
20	10	1989

ÚLTIMO PERIODO SABÁTICO DISFRUTADO, EN SU CASO

	DÍA	MES	AÑO		DÍA	MES	AÑO	No. DE MESES
DEL	23	03	2021	AL	22	03	2022	12

FECHA DEL PERIODO SABÁTICO SOLICITADO:

	DÍA	MES	AÑO		DÍA	MES	AÑO	No. DE MESES
A PARTIR DEL	24	03	2025	AL	23	03	2026	12

(PARA SER LLENADO POR LA OFICINA DEL CONSEJO DIVISIONAL)

APROBADO POR EL CONSEJO DIVISIONAL CON EL ACUERDO _____ DE LA SESIÓN _____

DOCUMENTOS QUE ACOMPAÑAN LA SOLICITUD:

- CONSTANCIA OFICIAL DE SERVICIOS EN LA UNIVERSIDAD ✓
- PROGRAMA DE ACTIVIDADES ACADÉMICAS A DESARROLLAR ✓

INTERESADO

DRA. CAROLINA CAMPOS MUÑIZ
FIRMA

APROBACIÓN DEL CONSEJO DIVISIONAL (PRESIDENTE)

DR. JOSÉ LUIS GÓMEZ OLIVARES
NOMBRE Y FIRMA

T1 SUBDIRECCIÓN DE PERSONAL
T2 ÁREA DE RECURSOS HUMANOS DE UNIDAD
T3 CONSEJO DIVISIONAL
T4 INTERESADO